Metrologia 18, 173–186 (1982)

metrologia

The Active Hydrogen Maser: State of the Art and Forecast

Jacques Vanier

Département de Génie Electrique, Université Laval, Québec G1K 7P4, Canada

Received: February 23, 1982 and in revised form May 19, 1982

Abstract

A general review of state-of-the-art hydrogen masers is presented. A description of the maser is made and the characteristics of state-of-the-art masers are given. Possible avenues of research are reviewed. Major fields where the maser finds application are mentioned. Finally, a list of laboratories involved in hydrogen maser development is given.

Introduction

In the field of atomic frequency standards, the active hydrogen maser [1] attracted much attention soon after its realization. This was due to its highly promising characteristics. Much work has been done on that maser and some 20 years after its invention a fair amount of research is still pursued on its basic physics as well as on its development. This work is done either in universities or in national laboratories of various countries.

The hydrogen maser, to be described here, is an active device or oscillator, in the sense that the atomic systems emit energy at a very definite frequency. It is a beam device which operates on the principle of storage of atoms in a bulb whose inside surface is coated with a special substance such as Teflon®. A beam of magnetically-selected atoms enters the bulb through a small hole and exits through the same hole. The bulb is placed inside a high-Q cavity tuned at the hyperfine resonance frequency of the hydrogen atoms which is 1,420 GHz. By limiting the motion of the atoms to a region of space where the field has a constant phase, first-order Doppler broadening is avoided. When special conditions are met on cavity Q and on relaxation times, the atoms emit their energy, part of which is then coupled out of the cavity by means of a small loop. The power output of the maser is of the order of 10^{-13} W. This is somewhat low but the spectral purity of the device is extremely high, due to a very low level of phase noise. Although several perturbations such as cavity pulling, magnetic-field bias, second-order Doppler effect, wall shift and others, affect the maser output signal, the frequency stability and accuracy of the maser are among the highest in the field of frequency standards. In present-day technology, the long-term frequency stability is controlled mostly by the frequency stability of the cavity while the accuracy is controlled by the wall shift.

Several general review papers have been written on the subject of atomic frequency standards during the last five years [2–4]. Those papers give general overviews of the characteristics of the standards. In the present text we shall limit ourselves to the hydrogen maser of the active type. We shall describe its general principles of operation, its state-of-the-art physical construction along with its characteristics. The main causes of its limitations in frequency stability and accuracy will be examined and possible avenues of research by which the maser characteristics could be improved will be mentioned.

I. Description of the Maser

The active hydrogen maser is an oscillator which obtains its energy from transitions in the ground state $2S_{1/2}$ of the hydrogen atom. This state consists of a manifold of 4 sub-levels. Under the influence of the electron-nucleus interaction, the sub-levels split into a triplet and a singlet, the latter level lying lowest. These two groups are identified by the quantum numbers $F = 1$ (highest) and $F = 0$ (lowest) [5]. Their unperturbed energy difference corresponds to the well-known 21 cm hydrogen wavelength or to the frequency, as measured against the primary ^{133}Cs $F = 3 \leftrightarrow F = 4$ transition, ν_H = 1,420,405,751.769 ± 0.002 Hz. This value was obtained by taking an average of all measurements reported, for which the wall-shift effect, to be discussed below, was determined at the same time as the frequency [6, 7]. In the presence of a magnetic field the degeneracy of the sub-levels is removed. The level structure is shown in Fig. 1 as a function of the applied magnetic field. The levels are identified by means of their F, m_F numbers, or with a simple notation by means of the numbers 1 to 4, starting from the highest energy; they are called Zeeman sub-levels.

The hydrogen maser operates between the levels $F = 1$, $m_F = 0$ and $F = 0$, $m_F = 0$ at a very low field of

0026–1394/82/0018/0173/$ 02.80

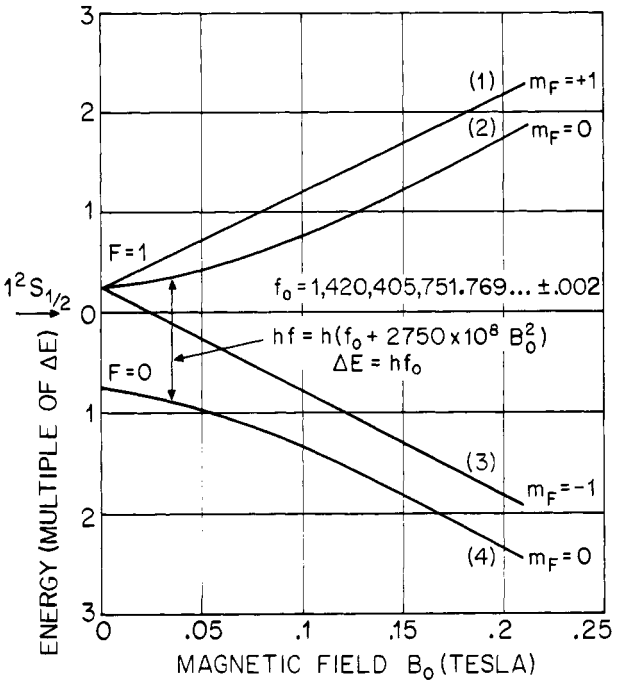

Fig. 1. Level structure of the ground state of the hydrogen atom as a function of the applied magnetic field

the order of 10^{-7} T. The output frequency of the maser is ν_H plus several positive or negative biases created by various perturbations which will be described later in this paper.

A schematic diagram of the maser is shown in Fig. 2. This is the so-called vertical type of construction and has generally been adopted by most scientists working actively in this field. The main reason for the vertical construction is the ease of assembly of all the parts, due to the cylindrical symmetry of the structure and the use of gravity to hold things together while assembly takes place.

A block diagram of the electronics associated with the maser is also shown in Fig. 2. These consist of two major items: 1) maser electronic controls as such, 2) receiver and phase-locked crystal oscillator.

1.1. The Maser

The maser, as shown in Fig. 2, can be described as follows. A beam of atomic hydrogen emerges from the dissociator. This beam is formed either through a single-hole capillary tube, 1 cm long, 0.5 mm in diameter or a multihole collimator 2 to 3 mm in diameter containing 400 to 800 tubes. Both methods produce approximately the same beam intensity. The second method seems to be

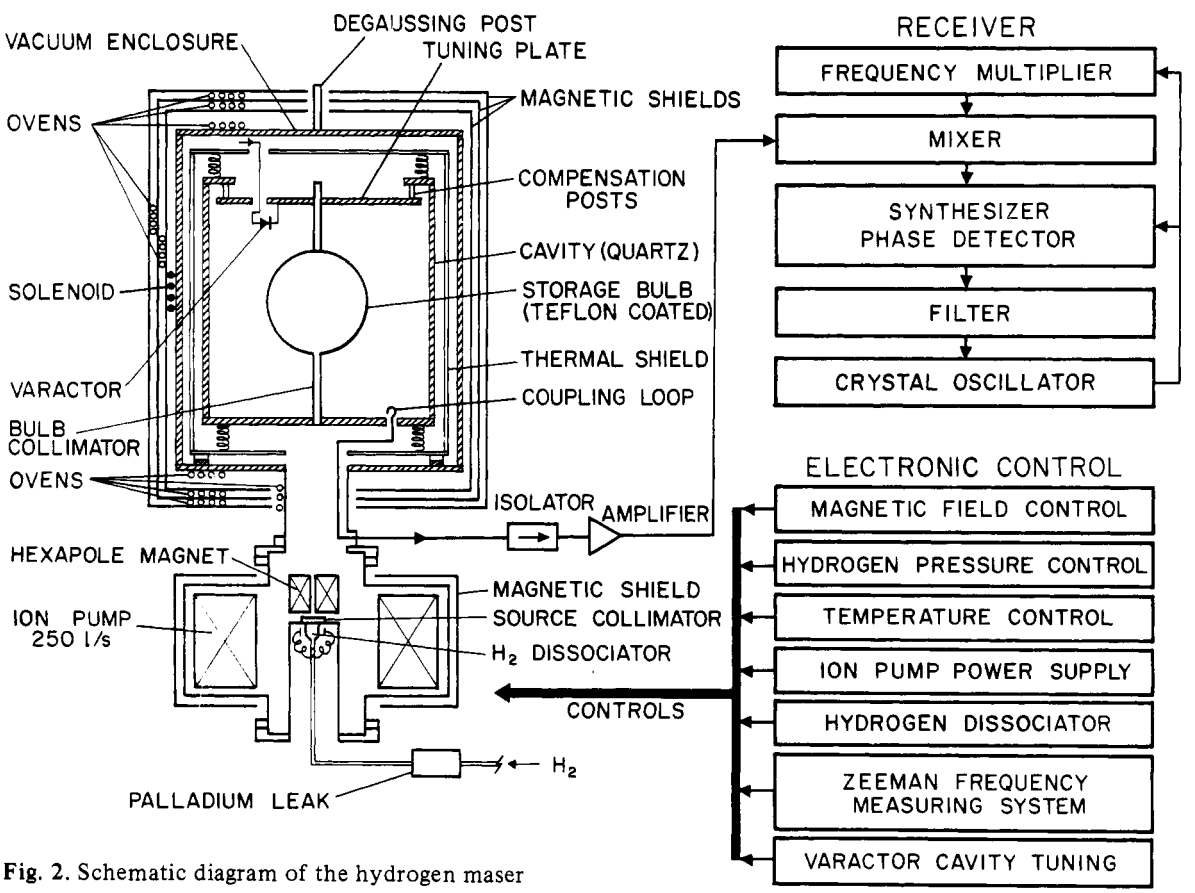

Fig. 2. Schematic diagram of the hydrogen maser

more effective in collimation but is less efficient at high beam intensities due, probably, to recombination in the collimator itself. Both techniques are widely used. The molecular hydrogen is generally obtained from a silver-palladium leak. Palladium has the property of being permeable to hydrogen, depending on its temperature. It is thus well adapted for servo-control through a heater driven by a feedback loop whose input command is a measure of the pressure in the source [8]. Atomic hydrogen is dissociated in a bulb by means of a rf field which produces a plasma. The power required is of the order of 5 W at a frequency of about 100 MHz. At the exit of the source, the beam enters the bore of an hexapole or a quadrupole magnet which acts as a spatial state selector. Its operation can be described as follows. The magnetic field is zero on the symmetry axis of the magnet, and increases radially towards the poles, to a maximum of about 0.5 T. The bore of the magnet is about 3 to 5 mm and the magnet itself is approximately 10 to 15 cm long. A beam of atomic hydrogen passing through this type of magnet is influenced in the following way. Those atoms in the two lowest energy levels 3 and 4 tend to go into the region of high magnetic field to reduce their potential energy. They are thus deflected away from the symmetry axis of the magnet where the field is strong. Those atoms in the higher states 1 and 2 have less energy when the field is weak. Consequently, they tend to go to the region near the symmetry axis of the magnet. In a sense, the magnet acts as a converging lens for those atoms in states 1 and 2 and as a diverging lens for atoms in states 3 and 4. A complete mathematical analysis of the function of the hexapole magnet can be found in [9].

After its exit from the magnet, the beam, composed mostly of atoms in levels 1 and 2, drifts towards the cavity and enters the storage bulb. The cavity, operating in the TE_{011} mode, is made of quartz or of other materials having a very low temperature coefficient of expansion. It is coated with silver on its inside. For an inner diameter of 28 cm the length required to make the cavity resonant at 1420 MHz, when the storage bulb is in place, is about 25 cm. The storage bulb is made of clear fused silica. It is possible to operate the maser with bulbs having diameters between 10 and 18 cm. The operation of the maser with different sizes of bulbs enables the experimenter to determine the bias introduced by the wall shift which will be discussed later. The inner surface of the bulb is coated with a thin film of Teflon®. The materials most commonly used are FEP 120 and TFE 42. These are long-chain polymers which inhibit relaxation of hydrogen atoms upon a collision. In fact, it is possible to obtain of the order of 10,000 collisions between an atom and the surface before relaxation takes place. The size of the exit hole of the bulb by which the atoms enter is adjusted so that an atom finds its way out after a time of the order of one second. This is approximately the lifetime of the atom before it relaxes on the wall. This exit hole may consist of a simple hole, a piece of tubing which acts as a collimator, or a multi-hole type of collimator. It is sometimes made of solid Teflon®. However, a Teflon®-coated piece of quartz is preferred since solid Teflon® may not have the same effect on the hydrogen-atom frequency as the film used in the bulb. Furthermore, solid Teflon® tends to outgas for long periods of time when placed under vacuum.

The arrangement, silver-coated quartz cavity plus quartz bulb, has an unloaded quality factor of the order of 50,000 to 60,000. The coupling factor of the output loop is adjusted to about 0.2, producing a loaded Q between 40,000 and 50,000. During their stay in the bulb the hydrogen atoms in level 2 fall into level 4 giving out their energy through stimulated emission produced by the rf field at 1.420 GHz which they create themselves. The whole system is maintained in a vacuum of the order of 10^{-5} to 10^{-4} Pa. This is realized by the use of one or two high-capacity vacuum pumps of the ion type.

The parts just described are the essentials of the hydrogen maser. However, in a practical device, especially in those of very high performance, many accessories are necessary. These include a minimum of three magnetic shields to reduce the effect of the ambient field and its fluctuations which affect the maser frequency in second order, a solenoid to produce a small magnetic field (10^{-7} T) parallel to the symmetry axis of the cavity, temperature-controlled ovens to stabilize the resonant frequency of the cavity, and excitation Zeeman coils for measuring the magnetic field by introducing transitions at the frequency between levels 1, 2 and 3. Since the maser output frequency depends slightly on the cavity tuning as will be explained later, the cavity is generally equipped with a fine-tuning device such as a small piston or a variable-capacitance diode, or both. These introduce a small reactance into the cavity without greatly affecting its quality factor. The tuning range is usually adjusted over a band of a few kHz.

1.2. The Maser Electronic Controls

The maser electronic controls consist essentially of five major parts. The circuit diagram of these various controls will not be given in detail. However, several references will be given where the reader will find ample details on their construction.

1.2.1. The Hydrogen Pressure Control. This control consists in general of a pressure transducer mounted in a bridge circuit, a power amplifier and a heater controlling the temperature of a palladium element permeable to hydrogen [8]. The general idea is shown in Fig. 3. In this arrangement, the transducer is a thermistor and the pressure desired is adjusted by setting the current flowing through the bridge. These controllers, due to time lags, tend to be unstable and special care must be taken in selecting the appropriate transfer function of the feedback loop. A short response time or small mass at the palladium leak helps to solve these problems. A fast-response palladium leak has been described by Viennet et al. [10]. When the maser is tuned according to the normal procedure to be described later, the frequency is independent of source pressure. Consequently, the

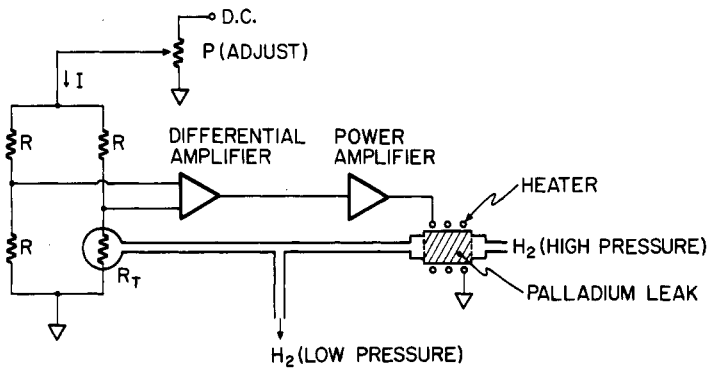

Fig. 3. A typical version of a hydrogen pressure control. This particular system uses indirect heating of the palladium filter and has a long time constant

stability required in the source pressure is not very high, except when the maser is being tuned.

1.2.2. The Magnetic-Field Control. In general this consists simply of stable current sources driving the main solenoid and the correction coils which may be needed to compensate for end effects. The current need not be known exactly since the magnetic field is measured through the Zeeman structure of the energy levels of the atoms. However, it should be very constant with time if extremely high stability is required. We shall discuss later the stability required for the field.

1.2.3. The Temperature Controls. Since the resonant frequency of the cavity has in general a temperature dependence which is rather difficult to cancel out completely by mechanical means, a good temperature control is required. This is done by ovens at several points on the maser as shown in Fig. 2. The sensors are thermistors and a standard bridge arrangement as shown in Fig. 4 may be used. Specially-selected low-drift thermistors are recommended. Barillet et al. [11] have described a temperature control with excellent characteristics.

1.2.4. The Zeeman Transition Generator. This unit is a simple variable low-frequency current source used to drive the Zeeman coils placed directly on the cavity. Five turns of fine wire, 20 cm in diameter are sufficient to excite the transitions. It is recommended that the oscillator be mounted directly on the maser together with a simple 4½-digit counter in order to determine the magnetic field exactly and to maintain a good record of its fluctuations.

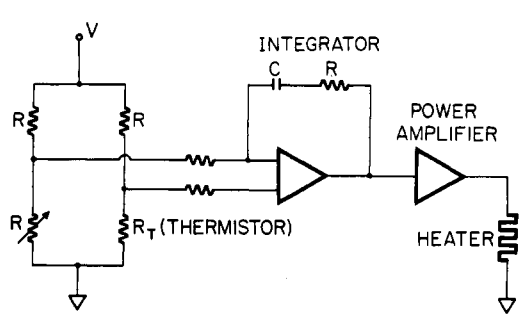

Fig. 4. A typical temperature control used in hydrogen-maser technology

1.2.5. The Radio Frequency H_2 Dissociator. About 5 to 10 watts are required at 100 MHz to produce high-efficiency H_2 dissociation. Circuits using vacuum tubes or transistors have been implemented successfully in the past [8, 12]. A typical oscillator circuit which has proved to be rather reliable is shown in Fig. 5. The transistor version is more delicate, due to changes in load impedance which take place when the discharge is started. The coupling of energy to the discharge can be done either in the electric or the magnetic mode. In the electric mode, two plates attached to the ends of the resonant circuit coil are in contact with the glass discharge bulb. In the magnetic mode, the glass discharge bulb is placed directly in the coil; it appears that the plasma acts as the secondary of a transformer whose primary is the coil of the resonant circuit. This last method of excitation is preferred. Coupling to the discharge is more efficient and the dissociator is more reliable. However, there is always some interaction with the glass enclosure. This last effect has caused, in the past, several problems of efficiency and of reliability. It has been studied by Ritz et al. [13].

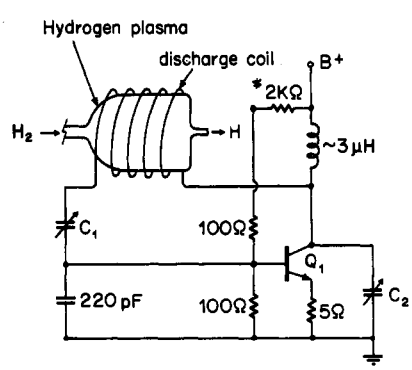

Fig. 5. Transistor oscillator used for molecular hydrogen dissociation. C_1 and C_2 are 5 to 15 pf variable capacitors. The transistor Q_1 is a high-frequency power transistor (~ 10 W). The dissociator coil may be made of 3 turns of heavy copper wire. The oscillation frequency is around 100 MHz. (* To be adjusted with Q_1)

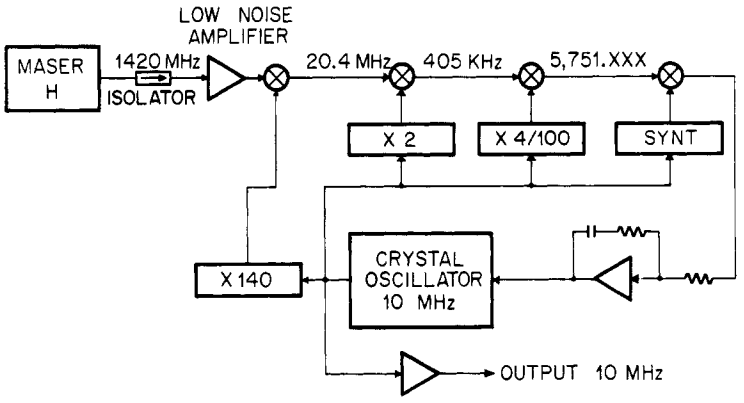

Fig. 6. Hydrogen-maser receiver. A crystal oscillator is phase-locked to the maser signal

In order to minimize this effect it is recommended to use a discharge bulb having a diameter in excess of 5 cm.

1.3. The Maser Receiver

The output frequency of the hydrogen maser is 1,420,405,751.xxx Hz. The last 3 digits depend mainly on the size of the bulb used and the magnetic field applied. The power output is of the order of 10^{-13} W. Consequently, a special receiver must be designed to bring the signal to a reasonable level and to make this signal appear at a usable frequency such as 5 or 10 MHz. Such a receiver is shown in Fig. 6 in the form of a block diagram [6]. In the case shown, the intermediate frequency is 20 MHz. The output at 10 MHz reflects the long-term stability of the maser; the short-term stability is in general that of the crystal oscillator itself. In some systems the receiver is mounted directly on the maser itself, while in others the receiver is an independent rack system. The use of an amplifier with a low noise figure (2–3 dB) as a first stage before the mixer at 1,420 MHz relaxes requirements on the noise figure of the receiver itself.

II. Basic Characteristics of State-of-the-Art H Masers

The theory underlying the operation of the hydrogen maser has been given by various authors [8, 14–16]. A large number of effects must be taken into account and it is best to consider them separately, depending on their influence on the oscillation condition or on the maser frequency.

2.1. Oscillation Condition

The oscillation condition of the maser can be calculated from the basic ideas found in general maser theory [17]. First, one calculates the power output of an ensemble of atoms, prepared in an excited state, submitted to a rf field and being perturbed by various relaxation mechanisms. One then calculates the power lost in the cavity either in the walls or in the coupling loop when such a rf field is present. The oscillation condition is obtained by equating these two powers. The power output P of the atomic ensemble is then given by [8]:

$$P/P_c = -2q^2\,(I/I_{th})^2 + (1-3q)\,I/I_{th} - 1, \tag{1}$$

where

$$P_c = \frac{\omega\hbar^2\,(\gamma_b+\gamma_w)^2\,V_c}{8\pi\mu_0^2\,Q_{c\ell}\eta} \tag{2}$$

$$I_{th} = \frac{\hbar V_c\,(\gamma_b+\gamma_w)^2}{4\pi\mu_0^2\,Q_{c\ell}\eta} \tag{3}$$

$$q = \frac{\sigma v_r \hbar(\gamma_b+\gamma_w)}{8\pi\mu_0^2(\gamma_b+\epsilon\gamma_w)}\,\frac{V_c}{\eta V_b}\,\frac{1}{Q_{c\ell}}\,\frac{I_{tot}}{I} \tag{4}$$

Here, the terms are defined as follows: σ is the spin exchange cross section, $\bar{v}_r$ is the relative velocity of the hydrogen atoms, $\hbar$ is Planck's constant over 2π, γ_b is the bulb escape rate, γ_w is the wall relaxation rate, V_c is the volume of the cavity, I_{tot} is the total atomic flux in atoms per second in states 1 and 2 entering the bulb, μ_0 is Bohr's magneton, $\epsilon\gamma_w$ is that part of the wall relaxation rate due to recombination and amounts to effectively increasing the escape rate γ_b, V_b is the bulb volume, $Q_{c\ell}$ is the loaded cavity quality factor, I is the atomic beam flux in state 2, ω is the maser frequency ν_m multiplied by 2π and η is the so-called filling factor defined as:

$$\eta = \langle H_z \rangle^2_{\text{bulb}} / \langle H^2 \rangle_{\text{cavity}}, \tag{5}$$

H being the rf field in the cavity. The factor q is the quality factor. For an oscillating maser the ratio P/P_c must be positive and the condition required on q is:

$$q \leqslant 0.172 \tag{6}$$

in which case, (1) has real roots. These roots are:

$$I^{\pm} = I_{th}\,\frac{(1-3q) \pm [1-3q)^2 - 8q^2]^{1/2}}{4q^2} \tag{7}$$

A plot of P/P_c versus I/I_{th} is shown in Fig. 7. With standard values encountered in practice such as $\eta V_c/V_b = 0.45$, $\gamma_b = 3\ s^{-1}$, $\gamma_w = 1\ s^{-1}$, $\epsilon = 1$, $\bar{v}_r = 3.58 \times 10^5$ cm/s, $\sigma = 2.85 \times 10^{-15}$ cm^2, $Q_{c\ell} = 3 \times 10^4$ and $I_{tot}/I = 2$ one obtains $q = 0.10$ and it is not difficult to obtain oscilla-

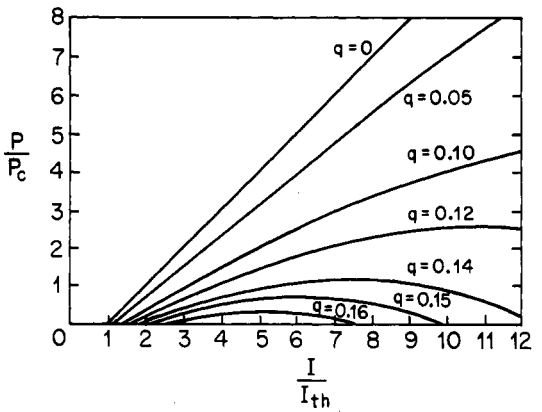

Fig. 7. Hydrogen-maser power P/P_c plotted against the flux I/I_{th} for various values of the quality factor (oscillating parameter) q

tion. With such a value of q, the maximum I/I_{th} of operation is very large and one is effectively limited only by the efficiency of the hydrogen dissociator and the speed of the pumps. With a flux about twice the threshold flux, a power of the order of 5×10^{-13} W is obtained. Although the theoretical results just given are based on a somewhat ideal situation, they describe quite well the operation of the maser as verified by several authors [18, 19].

2.2. *Relaxation Processes*

In the previous paragraph several relaxation processes were mentioned and from the equations given we have seen that they were important in controlling the maser output power. These relaxation processes can be divided into two types: 1) those which affect the population of the levels, 2) those which affect the coherence in the ensemble of oscillating atoms. These last relaxation processes have a direct effect on the resonance linewidth and, consequently, as will be discussed later, have an effect on the stability and in certain cases on the accuracy of the maser.

2.2.1. Escape Rate from the Bulb. This is a very important parameter. The value of this rate must be chosen according to the goal that is aimed at. A large escape rate (large bulb exit hole, short geometrical time constant) makes possible the realization of a very small quality factor q. This permits a very large range of operation in terms of I/I_{th}. Consequently, a large power output is possible with an increase in spectral purity as will be explained later. However, this may be gained only at the expense of a loss in long-term stability and a demand on vacuum-pump capacity due to the higher flux of operation required. Detailed methods of calculation of γ_b are given in reference [8] while pertinent data on gas flow are found in reference [20]. It is evident that due to the fact that atoms which exit through the bulb exit hole are lost, the effects of relaxation on both the population and the coherence are identical.

2.2.2. Wall Relaxation. Wall relaxation plays an important role in the operation of the maser. It acts somewhat differently both on the population (γ_{1w}) and on the coherence (γ_{2w}). Although a large amount of work has been done on this type of relaxation, it is not yet well understood what chemical or physical mechanisms are most important in the interaction between the atoms and the surface upon collision [21]. At present it appears that Teflon® surfaces (either FEP or TFE) give the smallest wall-relaxation rate. Rates less than 1 s^{-1} can be realized in bulbs with a diameter of the order of 15 cm. Consequently, wall relaxation does not, at present, inhibit the operation of the maser as an oscillator.

2.2.3. Spin-Exchange Relaxation. The effects of spin-exchange collisions in a hydrogen gas are fairly well understood [22–24]. It is well known that two atoms, entering into collision, can exchange electrons. This produces many effects. First, the populations of the two hyperfine levels $F = 0$, $m_F = 0$ and $F = 1$, $m_F = 0$ are affected by a relaxation rate equal to:

$$\gamma_{se_1} = n\bar{v}_r\sigma \,, \tag{8}$$

where n is the atomic density. Secondly, the coherence in the hydrogen gas, between the same pair of levels, is lost at the rate:

$$\gamma_{se_2} = \tfrac{1}{2}n\bar{v}_r\sigma \,. \tag{9}$$

This last mechanism produces a line broadening and is used to tune the maser cavity. These two effects can be controlled through the density n, itself controlled by the flux I and the bulb escape rate γ_b. They introduce the high-flux limit of operation of the maser when relaxation becomes incompatible with the oscillation condition. Finally, spin-exchange interaction produces a small frequency shift which will be discussed below.

2.2.4. Magnetic-Inhomogeneities Relaxation. The magnetic field existing at the site of the storage bulb may contain transverse (radial) components. Atoms moving through such a field may be submitted to a spectrum of radiation at the frequency corresponding to transitions of the $\Delta m_F = \pm 1$ type. The effect is to produce relaxation among the populations of the energy levels and to affect the coherence in the maser. These two effects have been studied theoretically and experimentally in some detail [19]. This type of relaxation can be made negligible by proper design of the solenoid and magnetic shields. An important design factor is the size of the neck hole in the maser shields. The smaller this hole is, compatible with the pumping speed required, the less chance there is of magnetic-inhomogeneity relaxation.

2.3. *Output Frequency: Accuracy and Long-Term Stability*

Stability is a measure of the degree to which the frequency will stay constant after the oscillator has been put into operation. On the other hand, accuracy can be defined, in simple terms, as the degree to which the frequency of the standard evaluated approaches, upon

calibration of the known perturbations, the internationally-accepted value for the frequency. This is done in terms of the second which is defined as the duration of 9,192,631,770 periods of the radiation corresponding to the transition between the hyperfine levels of the ground state of ^{133}Cs atoms.

In practice, the two concepts of stability and accuracy cannot be completely dissociated; sometimes they are connected through the same physical phenomena. In the present section, we shall discuss the effects which affect both the stability and accuracy of the maser. We shall attempt to separate them as much as possible but point out also their interdependence inside a given phenomenon.

2.3.1. Cavity Pulling. The cavity of the maser and the atomic ensemble form a coupled electromagnetic system. It is shown that the frequency ν_m of the maser depends on the resonant frequency of the cavity through the simple formula [15]:

$$\nu_m = \nu_0 + (Q_{c\ell}/Q_\ell)(\nu_c - \nu_0), \tag{10}$$

where ν_0 is the hyperfine frequency of the hydrogen atoms including the wall shift, the second-order Doppler effect and the magnetic-field bias; ν_c is the resonant frequency of the microwave cavity and Q_ℓ is the atomic line Q defined as:

$$Q_\ell = \nu_0/\Delta\nu_\ell \ . \tag{11}$$

$\Delta\nu_\ell$ is the width at half amplitude of the atomic resonance line. Relation (10) is not complete since it does not include the spin-exchange shift which will be discussed later. However, it is sufficient for the discussion of the cavity characteristics required for a given stability and accuracy of the maser frequency. The cavity Q is of the order of 40,000 while the line Q is close to 1.5×10^9 in standard designs. Somewhat higher line Q's can be achieved by using a large bulb and a small γ_b. Consequently, in general, a frequency pulling of the order of 0.027 Hz per kilohertz of cavity-resonance detuning is obtained. A cavity made completely of quartz has a temperature coefficient of the order of 1 kHz/°C. On the other hand a Cervit® cavity, in principle, can be designed with a zero temperature coefficient. However, the introduction of the storage bulb into the cavity drastically changes its electrical characteristics. Actually, even though its loss-tangent is very small, not significantly affecting the cavity Q, the quartz bulb has a dielectric constant which changes the cavity resonance frequency by several megahertz. Furthermore this dielectric constant is temperature dependent. Thus, finally, with any type of cavity, one is forced into some kind of cavity compensation or else accepts a residual temperature coefficient for the whole structure. A coefficient below 1000 Hz per degree Celsius is easily achieved. With the above figures, this gives a maser-output-frequency temperature dependence < 0.027 Hz/°C. This corresponds to about 2×10^{-11} per °C. In order to achieve a stability of 1×10^{-14}, one requires a temperature stabilization better than one millidegree. This can be achieved over medium times. In the long-term region it appears that one is dependent upon the stability of the temperature sensor used in the temperature control. In general, thermistors are used and stability of the order of 0.01 °C per year appears to be the limit of present-day technology. In practice, it appears possible to obtain over 20 days a temperature stability compatible with a maser stability of 5×10^{-14} [11]. On the other hand, problems related to the mechanical stability of the materials and their contacts should not be overlooked as a possible source of long-term frequency drift. Materials that have different coefficients of expansion may have a tendency to slip on each other in an erratic manner under the influence of temperature fluctuations. This effect may cause frequency jumps, which can be avoided by using a proper design and a proper choice of materials in contact.

The dependence of the degree of pulling of the cavity tuning upon the line Q makes possible a tuning of the cavity by spin-exchange broadening. Actually, automatic tuning devices have been realized which rely directly on this phenomenon [12, 25–27]. In these devices, the line Q is altered in sequences. The maser frequency, relative to another source whose frequency does not need to be known, is measured for two values of the line Q. The difference between these two measurements is used as an indication of the amount as well as the sign of the cavity detuning relative to the oscillation frequency of the hydrogen atoms. The information obtained is then processed, transformed into an error signal and sent to the varactor controlling the cavity resonance frequency. The increase in very-long-term stability is generally obtained at the expense of slight losses in medium-term stability due to the perturbation introduced by the alteration of the line Q and due to the corrections applied to the varactor. In principle, with such a device, no long-term drift due to cavity mis-tuning should be observed. A theory covering the subject of autotuning systems has been developed [28]. A stability better than 1.5×10^{-14} over 5 days has been observed [25, 27]. This is to be compared to a stability of 3 to 5×10^{-14} for the same period of time as observed for the same masers not being tuned automatically. It should be realized, however, that this improvement is obtained at the expense of a fair amount of complexity, that autotuners are still laboratory devices and are much discussed either for their effectiveness or their reliability. Not enough data are available yet to draw final conclusions on this subject.

Accuracy: the cavity tuning affects the accuracy of the maser, through the fact that the exactness of this tuning can be done only within certain limits. These limits are functions of the maser stability during the time of the tuning process itself and of the amount of broadening possible through spin exchange interactions. In the so-called classical method of tuning, the difference between the frequency of the maser to be tuned and another stable source is measured for two beam intensities. The frequency of the other source does not need to be known but must be stable.

Actually, the residual offset δ_{offset} after tuning, using (10) is given by [29]:

$$\frac{\delta_{\text{offset(LP)}}}{\nu_0} = \frac{(\nu_{\text{mLP}} - \nu_{\text{mHP}})}{\nu_0} [1 - Q_{\ell\text{HP}}/Q_{\ell\text{LP}}]^{-1}, \quad (12)$$

where $(\nu_{\text{mLP}} - \nu_{\text{mHP}})$ is the difference in frequency of the maser for low and high hydrogen pressures in the storage bulb (or low and high beam fluxes) and, $Q_{\ell\text{LP}}$ and $Q_{\ell\text{HP}}$ are the low-pressure and high-pressure line Q's possible. Obviously, if $(\nu_{\text{mLP}} - \nu_{\text{mHP}})$ can be measured exactly there is no residual offset after tuning. However, the precision on the measurement of this quantity is a function of the stability of the maser during the time of the measurement. In practice, it can be measured to approximately 10^{-14} with good masers. One then sees that the value of δ_{offset} is a function of the ratio of the line Q at low and high pressures. If $Q_{\ell\text{LP}}/Q_{\ell\text{HP}}$ can be made of the order of 2, then $\delta_{\text{offset}}/f_0$ becomes 2×10^{-14} for the measurement precision quoted above. This number is approximately what is found in practice when a maser is tuned repeatedly [29].

Great care should be taken in the design of the cavity in order to avoid problems related to the effect of pulling. All parts should be firmly joined together and the use of any material which has a tendency to flow should be avoided. All thermal parts should be reduced in order to avoid temperature fluctuations and gradients. The cavity should be decoupled from the bell-jar's bottom in order to prevent barometric fluctuations from affecting its frequency. The effect takes place through the deformation of the bell-jar's base-plate. This induces strain in the cavity and results in a frequency shift. One solution consists in supporting the cavity, on a false bottom attached to the bell-jar's base-plate at a point where deformations are small (near the neck tubing). The use of tuning pistons should be avoided if possible, because of thermal problems and mechanical instabilities. A varactor diode placed directly in a loop in the cavity presents a reactance which varies with the inverse of the voltage applied and can be used for fine tuning of the maser [30]. Finally, the coupling loop should be designed very carefully, since it acts as an added reactance and alters the resonant frequency of the cavity. An isolator with minimum reflexion (low VSWR), well controlled in temperature and shielded against magnetic-field fluctuations, which can affect its characteristics, should be used at the cavity output. It is recommended that this isolator be followed by a preamplifier at 1,420 MHz also controlled in temperature. The positions of the isolator and of the preamplifier can be interchanged on the condition that the input impedance of the amplifier stays constant with time. It is only through this great care that one can hope for long-term stability in the 10^{-14} range and better.

2.3.2. Spin-Exchange Interactions. Spin-exchange interactions between hydrogen atoms strongly affect the maser. First, as discussed in section 2, they broaden the resonance line, thus permitting a modulation of the line Q, an effect which is used for tuning the maser cavity as described above. Secondly, they create a small frequency shift [22–24]. Fortunately, the large part of this frequency shift is proportional to the population difference between the two levels involved in the maser oscillation. Analysis shows that the method of tuning the cavity, described above, sets the cavity off the atomic resonance by an amount such that this part of the spin-exchange shift is cancelled. This phenomenon has also been verified experimentally [31, 32]. The other part of the spin-exchange shift is much smaller than the first one and is not proportional to the population difference [33]. It can thus introduce a small frequency shift which depends on the maser's physical configuration. The maser angular frequency ω, including these two effects and the cavity pulling, is given by [34]:

$$(\omega - \omega_0) = (1/T_2)\,(2\Delta\nu_0/\delta\nu_c - C\lambda) + \epsilon_H/T_H\,, \quad (13)$$

where ω_0 is equal to $2\pi\nu_0$; $\Delta\nu_0$ stands for $(\nu_c - \nu_0)$, $\delta\nu_c$ is the width of the cavity resonance; T_2 is the transverse relaxation time of the atomic transition; $(T_H)^{-1}$ is the part of the relaxation rate due to H-H collisions; the parameter C includes several physical constants as well as actual maser parameters; λ is the spin-exchange-frequency-shift cross section and ϵ_H is a parameter which represents the effect of interruption of the oscillating magnetic moments during collisions. The value of λ has been measured as a function of temperature [34]. On the other hand, only one experimental determination of ϵ_H has been reported [33]. It would be desirable that other measurements be made, especially as a function of temperature.

When the maser is tuned by the method described above, the major part of the spin-exchange frequency shift is cancelled by a slight mistuning of the cavity. However, the method does not compensate for the effect of ϵ_H and a small residual spin-exchange shift is present. The tuned frequency of the maser ω_t is given by

$$\omega_t - \omega_0 = -2\,\epsilon_H/T_2', \quad (14)$$

where T_2' represents that part of the transverse relaxation rate which is not due to H-H collisions. The value of ϵ_H is of the order of -4×10^{-4} at the normal temperature of operation of the maser [35]. With a T_2' of the order of 0.5 s one obtains a frequency shift of 1.6×10^{-4} Hz. Thus, to minimize the effect the maser bulb should have a long geometrical time constant. However, ϵ_H is known to about 10%. Thus the effect can be calculated with an accuracy of approximately 2.6×10^{-14}. This is of the order of magnitude of the maser tuning accuracy. Although ϵ_H depends on the temperature, it is not expected to affect the stability of the maser due to its small absolute value and the temperature stability under which masers are normally operated.

2.3.3. Magnetic-Field Bias. The hydrogen maser operates normally in a magnetic flux density of the order of 10^{-7} T. The average value of this flux can be measured easily through a slight perturbation introduced at the frequency of the Zeeman transitions. The magnetic flux density is related to this frequency by the relation:

$$\nu_Z = 1.400 \times 10^{10} < B_Z >. \quad (15)$$

On the other hand, the maser frequency is related to the magnetic flux through the relation:

$$\nu_m = \nu_0 + 2.752 \times 10^{10} B_z^2. \quad (16)$$

It is standard practice to take B_z^2 as $< B_z >^2$ and write:

$$\nu_m = \nu_0 + 1.417 \times 10^{-9} \nu_Z^2. \quad (17)$$

This procedure normally introduces a negligible error. A flux density of 5×10^{-7} T gives a ν_Z of 7×10^3 Hz and a maser frequency shift of 0.07 Hz or 5×10^{-11}.

Accuracy: the precision to which the value of ν_Z can be determined depends on the stability and homogeneity of the magnetic field. Normally, in a well-designed maser, the field is homogeneous enough that a Zeeman-transition linewidth of the order of 1 Hz is obtained. The precision in determination of the Zeeman frequency is then only a function of the field stability. This is a function of the stability of the current source driving the solenoid and of the quality of the magnetic shielding used. In practice, with four well-designed magnetic shields and a standard regulated current source it is possible to obtain a precision in ν_Z of a few hertz. The uncertainty in the determination of the maser frequency is then given by:

$$\Delta\nu_m = 2.8 \times 10^{-9} \nu_Z \Delta\nu_Z \quad (18)$$

With an uncertainty of 2 Hz on $\Delta\nu_Z$ for ν_Z equal to 7 kHz one obtains $\Delta\nu_m = 3.9 \times 10^{-5}$ Hz or 2.8×10^{-14}. Obviously the error can be reduced by operating at a lower magnetic field.

However, at too low fields, another effect takes place due to the importance of residual field inhomogeneities in the cavity environment. These inhomogeneities can originate from residual hard spots in the magnetic shields as well as from leakage of external fields through apertures required for the passage of the pumping duct, holders and electrical connections. The combined effect of dc and rf field gradients produces a shift in the maser output frequency [35]. This shift is proportional to the population difference of levels (1) and (3) shown in Fig. 1, and to the field gradients. The effect is a function of the actual design of a particular maser and, in a typical case, may be of the order of several parts in 10^{13} at a field of 10^{-7} T [2]. Consequently, it could affect the accuracy of the maser. It can be minimized by proper shield design and by careful centering of the storage bulb in the cavity. Its effect can also be reduced by operating the maser at high magnetic fields. The size of field required is best determined experimentally. Finally, it is also possible to make the effect negligible by equalizing the populations of levels (1) and (3) [36].

Stability: in practice, it is found that with well-designed magnetic shields (4 to 6 layers made of μ-metal® or Moly-permalloy® material) the shielding factor is sufficiently large [37, 38] and stability of the magnetic field is not a limitation on the frequency stability of the maser [39].

2.3.4. Wall-Shift Bias. Much work has been done on the measurement of the wall shift and still more has been written on its properties [6, 7, 21, 40–43]. It originates from a perturbation of the hydrogen atom's wave function upon collision with the surface of Teflon® covering the inside of the storage bulb. Its value is given by [40]:

$$\Delta\nu = (W/D)\,(1 - a[t - t_0]), \quad (19)$$

where D is the diameter of the bulb, t is the temperature of operation of the maser, W is the wall-shift parameter at temperature t_0 and a is the temperature coefficient. W is of the order of (-421 ± 40) mHz cm and a is about $(-19.8 \pm 4)\ 10^{-3}\ K^{-1}$ for TFE 42. On the other hand, for FEP 120 the value is of the order of (-355 ± 25) mHz cm while a is $(-11.9 \pm 1)\ 10^{-3}\ K^{-1}$ [42]. The value of the wall shift goes through zero at about 85 °C [7, 21, 45, 46].

A review on the subject has been published [44]. The main conclusion drawn is that W can be predicted only within certain limits. In practice, one has to make measurements of the maser frequency with bulbs of various diameters with a given batch of Teflon®. Even when this is done, it is not possible to obtain an accuracy much better than 10%. This limits the actual accuracy of the maser to about 1 to 2×10^{-12}. It appears that it is only with a radical change in the storage bulb design that an improvement in the accuracy of the maser can be expected. A variable-volume storage bulb [47, 48], operated at the temperature where the wall shift vanishes, appears to be the goal to aim for [45, 46, 49]. However, such bulbs have been operated only as laboratory models and it appears that mechanical problems associated with the movement of parts or membranes inside a cavity are not yet entirely solved. With a good bulb design, one may hope for an increase in maser accuracy to the order of a few parts in 10^{13}. On the other hand, the stability of the wall shift with time raises questions. Experiments have been done with bulbs over several years and changes of the order of 3 to 8×10^{-13} per year have been detected [50]. More experiments need to be done before any definitive conclusions can be drawn. Experiments should be repeated with masers of a design different from that of the ones used in [50].

2.3.5. Second-Order Doppler Effect. The second-order Doppler effect produces a frequency shift of the hyperfine transition proportional to the temperature. The value of this shift is [15]:

$$\Delta\nu_D = 1.957 \times 10^{-4}\ T, \quad (20)$$

where T is the absolute temperature.

At a temperature of 313 K one has:

$$\Delta\nu_D = 4.314 \times 10^{-11}\ \nu_m \cong 0.06 \text{ Hz}.$$

This shift is rather large. But since it is linear with temperature, a knowledge of the latter to 0.1 K gives an accuracy in ν_m better than 2×10^{-14}.

2.4. Maser Short Term Stability

The statistical properties of the frequency fluctuations of the maser can be characterized in several ways [51]:

a) the one-sided spectral density $S_y(f)$, in units of Hz^{-1}, of fractional frequency fluctuations $y(t)$, where f is a Fourier frequency component.

b) the phase spectral density $S_\phi(f)$ in units of rad^2/Hz,

c) the two sample variance, $\sigma_y^2(\tau)$, where τ is the time during which the frequency is measured.

All these methods of characterization are related to each other in the following manner:

$$S_y(f) = (f^2/\nu_0^2)\, S_\phi(f), \tag{21}$$

$$\sigma_y^2(\tau) = 2\int_0^{f_h} S_y(f)\, \frac{\sin^4 \pi f\tau}{(\pi f\tau)^2}\, df, \tag{22}$$

where ν_0 is the oscillator frequency and f_h is the filter cut-off frequency in the measurement set up. In the hydrogen maser, $S_y(f)$ results from various contributions [52, 53]. These are:

a) $$|S_y(f)|_{add} = h_2 f^2, \tag{23}$$

where h_2 is a factor determining the size of $S_y(f)$ at a Fourier frequency of 1 Hz. This is the part of the spectral density which results from the thermal noise added to the maser signal. This noise may be generated either in the cavity or in the microwave receiver. It has an f^2 dependence and gives rise to white phase noise. In the time domain it gives rise to a $\sigma_y^2(\tau)$ of the following form:

$$\sigma_y^2(\tau)_{add} = \frac{kT\omega_R\, Q_{ext}}{P_b \omega_0^2\, Q_{c\ell}^2 \tau^2} = h_2 \frac{3\omega_R}{(2\pi)^3\, \tau^2}, \tag{24}$$

where F is the noise figure of the receiver, ω_R its bandwidth, Q_{ext} the external Q, $Q_{c\ell}$ the loaded Q of the cavity and P_b is the power delivered by the beam.

b) $$|S_y(f)|_{int} = h_0\,. \tag{25}$$

This is white frequency noise intrinsic to the maser whose amplitude is characterized by the factor h_0 and which originates from a modulation of the maser signal by the noise itself. It is independent of frequency and, in the time domain, it gives rise to a $\sigma_y^2(\tau)$ of the form:

$$\sigma_y^2(\tau) = \frac{kT}{2P_b Q_\ell^2 \tau} = h_0\, \tau^{-1}. \tag{26}$$

c) $$|S_y(f)|_{r.w.} = h_{-2}\, f^{-2}. \tag{27}$$

This term is referred to as a random-walk frequency contribution; its amplitude is characterized by the factor h_{-2}. It probably originates from fluctuations of the cavity resonant frequency. It has a f^{-2} dependence and gives rise, in the time domain, to a $\tau^{1/2}$ variation of $\sigma(\tau)$ vs τ.

$$\sigma_y^2(\tau) = h_{-2}\, 2\pi^2 \tau/6. \tag{28}$$

d) $$|S_y(f)|_{f\ell} = h_{-1}\, f^{-1}. \tag{29}$$

This term represents a flicker noise of frequency. Its contribution, however, has not yet been established with certainty. It has an f^{-1} dependence and, if present, would give rise to a plateau in the curve of $\sigma(\tau)$ versus τ, in the time domain.

$$\sigma_y^2(\tau) = h_{-1}\, 2\ell n 2. \tag{30}$$

What is generally observed in practice is a valley in the $\sigma_y(\tau)$ graph and no conclusions can be drawn relative to the presence of flicker noise of frequency.

Contributions a) and b) are the most important ones in the so-called short-term region. The presence of white phase noise is generally observed, while the contribution from white frequency noise is seen in masers having good long-term frequency stability [54]. The presence of large fluctuations originating from random-walk processes or drift may mask the white frequency noise contribution.

A typical maser would have a characteristic as shown in Fig. 8. The region of $\sigma(\tau)$ above 10^3 s is a function of the quality of the design of the particular maser. From the data reported in [54], we can write:

$$S_y(f) = 7.5 \times 10^{-36} f^{-2} + 2.6 \times 10^{-27} + 7.1 \times 10^{-26} f^2, \tag{31}$$

which defines the parameters h_{-2}, h_0 and h_2, for the particular maser studied.

Attempts could be made to improve the f^2 dependence of $S_y(f)$ or the short-term stability, by increasing the power output of the maser. However, there are limitations to this. First, large cumbersome pumps would be needed in order to cope with the intense beam flux necessary. Secondly, in order to increase the power, the bulb's geometrical time constant needs to be made short, which reduces the line Q and the long-term frequency stability.

In fact, the optimum power illustrated in Fig. 8 is given by:

$$P_{opt} = (P_c/8)\, |1/q^2 - 6/q + 1|\,. \tag{32}$$

In the case where wall relaxation is not too important, (2) and (4) show that q is independent of γ_b while the power P_c is proportional to the square of γ_b.

In that case, the optimum power becomes:

$$P_{opt} = K_1\, \gamma_b^2, \tag{33}$$

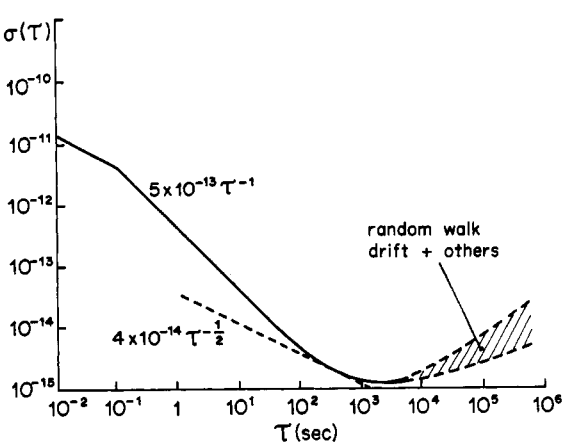

Fig. 8. Frequency stability of a typical hydrogen maser

where K_1 is a constant which depends only on the maser physical characteristics and fundamental constants.

On the other hand, the linewidth $\Delta\nu$ is equal to γ_2/π or approximately γ_b/π. The line Q is then given by:

$$Q_\ell = (K_2\ \gamma_b)^{-1}, \tag{34}$$

within the same approximations as those made above. K_2 is equal to $\nu_0\pi$.

Thus, within this framework, the contribution originating from noise within the maser linewidth as given by (26) is a constant, quite independent of the maser power output. It sets a lower limit on the maser stability. This limit is approximately:

$$\sigma_y^2(\tau) = (kT/2)\,(K_2^2/K_1)\,(1/\tau). \tag{35}$$

We evaluate the constants for a typical maser and we obtain:

$$\sigma_y\,(\tau) \cong 4 \times 10^{-14}\ \tau^{-1/2}. \tag{36}$$

On the other hand, the reduction in line Q resulting from an increase in γ_b makes the maser frequency more sensitive to changes in environmental conditions, especially temperature. This normally results in an increase in medium-term frequency fluctuations and a rise in the value of $\sigma(\tau)$, for averaging times larger than 10^3 s. The problem has been studied in detail in [54] and [55].

Consequently, a compromise must be accepted and normally the time constant of the bulb is adjusted to such a value that the line Q is of the order of 1 to 2×10^9.

2.5. Phase-Locked Crystal Oscillator

In practice, as described in Sect. I–1.3, a quartz-crystal oscillator is locked to the maser frequency. The overall response of the system is given by [53]:

$$[S_y\,(f)]_{q\ell} = \left[\frac{1}{1+G\,(f)}\right]^2 [S_y\,(f)]_{qf} - \frac{1}{n^2}\left[\frac{G(f)}{1+G(f)}\right]^2 [S_y\,(f)]_m, \tag{37}$$

where the subscripts m, qℓ, qf, mean respectively: maser, quartz locked and quartz free; n is the ratio of the maser frequency to the quartz-crystal-oscillator frequency. $G(f)$ is given by:

$$G(f) = n\,SC\,(2\pi jf)^{-1}\,F(f), \tag{38}$$

where S is the sensitivity of the quartz-crystal frequency control to an applied correction voltage in rad s^{-1} V^{-1}, C is the characteristic of the phase detector in V rad^{-1} and $F(f)$ is the transfer function of the filter which follows the phase detector. Since it is possible to construct quartz oscillators with rather good short-term stability (or good spectral purity) it is common practice to set the servo-loop response such that the quartz oscillator is left unaffected for frequencies greater than about 10 Hz. Then, the overall response is such that, in the short term, the frequency fluctuations are those of the free-running crystal oscillator, while in the long term the maser stability is transferred to the crystal oscillator. The behaviour of quartz oscillators locked to masers has been studied in detail in [56] while a review of the subject describing the implementation of various systems is given in [57].

III. State of the Art and Future Avenues of Research

There are several laboratories involved in research and development in the field of hydrogen masers. A list of those laboratories is given in the Appendix, along with principal references where a comprehensive description of their work is given.

As far as frequency stability is concerned, it appears that the limit set by white frequency noise has been reached [54]. A frequency stability of 8×10^{-16} has been observed for an averaging time of 1 h. In the short-term region, the stability is limited by the presence of white phase noise. It is approximately 5×10^{-13} for a 1 s averaging time in a 3 Hz bandwidth. These observations apply to masers operating near room temperature. On the other hand, in the long-term region, the causes of instability cannot be identified as clearly. The size of the fluctuations depends very much on the particular design used. These fluctuations, however, originate in most cases in cavity instabilities as described previously. In fact, in standard types of construction a fractional frequency stability of one part in 10^{15} requires, from the cavity, a frequency stability of 0.05 Hz at 1.4 GHz. The dependence of the cavity frequency on its length is of the order of 10 MHz/cm. Consequently, the 10^{-15} frequency-stability requirement means a cavity-length stability of about 50 pm. This is an extremely severe requirement on mechanical stability, especially in the present case, since the cavity is made of different parts held together by springs or other means.

In the very-long-term region it appears that the wall-shift stability may be a problem since drifts of the order of 3×10^{-13} per year have been observed [50].

Nevertheless, several laboratories are engaged in a program of research aimed at an improvement of the short- and medium-term stability of the maser. This research is oriented towards a lowering of the temperature of operation of the maser. Experiments are being performed at temperatures down to 4.2 K, the normal boiling point of liquid helium [54]. A maser has been operated at temperatures as low as 25 K [58]. Fundamental work is also performed on magnetic resonance of atomic hydrogen at temperatures as low as 1 K [59–61]. It is expected that a maser operating at a temperature below 25 K would have a fractional frequency stability better than 10^{-16} for an averaging time of 10^3 s. Several problems, however, arise from these low temperatures of operation. It appears that the wall coating suffers from a contamination originating from a condensation of residual gases in the system [58]. This difficulty could be bypassed by a continuous dynamic recoating of the storage bulb.

In the long-term region it appears that the mechanical stability of the cavity sets the limit. Consequently, a different approach has to be taken. The technique of autotuning based on spin-exchange broadening should, in principle, solve the problem. An analysis of the perform-

ance of these systems has been reported recently [62].

In the very long term, a study of various masers will be required before a definite conclusion can be drawn concerning the drift observed. It is very likely that the wall-shift characteristic of Teflon® itself varies with time, but the possibility exists that the observed drift is caused by contaminants in the vacuum system.

As far as accuracy is concerned, it appears in general that the limit is set by the uncertainty in the wall-shift determination. However, Petit et al., using a variable-volume storage bulb, claimed an accuracy of 6×10^{-13}, the main uncertainty originating from cavity tuning and offsets from steady-state temperature. Nevertheless, storage bulbs with variable volume have not lived up to expectations. Wall-shift homogeneity over the surface of the bulb, mechanical stability of moving parts inside the cavity and magnetic-inhomogeneity shifts remain the major problems to be solved [49]. Operation at the temperature where the wall shift vanishes still appears to be attractive [45, 49].

In the standard configuration the size of the maser is determined by the cavity which operates in the TE_{011} mode. Other configurations have been proposed. For example a maser operating with a TE_{111} cavity has been realized [63]. This cavity is approximately half the size of the conventional TE_{011} cavity. Other cavity modes have been proposed and are under study [64–66]. It is believed that the successful operation of these cavities will lead to a drastic decrease in the size of the maser.

IV. Applications

At present, the principal uses of hydrogen masers have been in:

1. fundamental research leading to a better understanding of spin-exchange, atom-surface interactions, and relaxation phenomena in general [19, 21, 22, 24, 34, 35, 54],
2. space navigation and tracking [67–69],
3. radio astronomy, very-long-baseline interferometry (VLBI) [70, 71],
4. techniques of VLBI used for geodesy [72, 73] and clock synchronization [74, 75],
5. techniques of oscillator transfer as a stable reference-frequency source [76],
6. time-keeping [77],
7. experiments to verify some fundamental concepts of relativity [78].

Appendix

Laboratories Involved in Research and Development in the Field of Hydrogen Masers

The present list is intended to be as complete as possible. It is possible, however, that laboratories active in the field have escaped the attention of the author.[1] The numbers in brackets are the main references in which the laboratories involved have described their recent work.

Laboratoire de l'Horloge Atomique, Orsay, France [79]
NASA Goddard Space Flight Center, USA [80, 81]
Johns Hopkins Applied Physics Laboratory, USA [80, 81]
Sigma Tau Corporation, USA [65]
Smithsonian Astrophysical Laboratories, USA [82]
National Research Council, Canada [50]
Laboratoire d'Electronique Quantique, Université Laval, Quebec, Canada
Jet Propulsion Laboratory, Pasadena, CA. [67]
Hughes Research Laboratories, USA [66]
Shanghai Bureau of Metrology, China [43]
Shanghai Observatory, China [83]
Wuhan Institute of Physics, China [84]
Radio Research Laboratories, Japan [85]
Williams College, USA [60, 61, 86]
National Physical Laboratory, England [87]
Institut de Physique, Bucarest, Romania [88]
Gosstandard, USSR [89]
Azulab, S.A., Switzerland [90]
CSIRO, Australia [91]

[1] The author apologizes for such omissions if any

References

1. H.M. Goldenberg, D. Kleppner, N.F. Ramsey: Phys. Rev. Lett. **5**, 361–362 (1960)
2. C. Audoin, J. Vanier: J. Phys. E. Scient. Instr. **9**, 697–720 (1976)
3. J. Vanier: Atomic frequency standards: Survey and forecast. Proc. 9th Annual Precise Time and Time Interval (PTTI) Applications and Planning Meeting, pp. 9–58, 1977. (NASA, Goddard Space Flight Center, Greenbelt Md)
4. H. Hellwig: Radio Science **14**, 561–572 (1979)
5. N.F. Ramsey: Molecular beams. Oxford: Oxford Clarendon Press 1955
6. J. Vanier, R. Larouche: Metrologia **14**, 31–37 (1978)
7. P. Petit, M. Desaintfuscien, C. Audoin: Metrologia **16**, 7–14 (1980)
8. D. Kleppner, H.C. Berg, S.B. Crampton, N.F. Ramsey, R.F.C. Vessot, H.E. Peters, J. Vanier: Phys. Rev. **138A**, 972–983 (1965)
9. C. Audoin, M. Desaintfuscien, J.P. Schermann: Nucl. Instrum. Methods **69**, 1–10 (1969)
10. J. Viennet, P. Petit, C. Audoin: J. Phys. E. Scient. Instr. **6**, 257–261 (1973)
11. R. Barillet, J. Viennet, P. Petit, C. Audoin: J. Phys. E. Scient. Instr. **8**, 544–545 (1975)
12. H.E. Peters, T.E. McGunigal, E.H. Johnson: Hydrogen standard work at Goddard Space Flight Center. NASA Report, X523-68-152, May 1968
13. V.H. Ritz, V.M. Bermudez, V.J. Folen: Analysis of degraded hydrogen dissociator envelopes by AES. Proc. 9th Annual Precise Time and Time Interval (PTTI) Applications and Planning Meeting, pp. 353–369, 1977. (NASA, Goddard Space Flight Center, Greenbelt, Md)
14. C. Audoin, J.P. Schermann, P. Grivet: Physics of the hydrogen maser. In: Advances in Atomic and Molecular Physics, Vol. 7, D.R. Bates, I. Estermann (eds.) pp. 1–45. London: Academic Press 1971
15. D. Kleppner, H.M. Goldenberg, N.F. Ramsey: Phys. Rev. **126**, 603–615 (1962)
16. J. Vanier: Basic theory of lasers and masers. New York: Gordon and Breach Science Publishers 1971

17. K. Shimoda, T.C. Wang, C.H. Townes: Phys. Rev. **102**, 1308–1321 (1956)
18. C. Audoin, M. Desaintfuscien, J.P. Schermann: C.R. Acad. Sci. (Paris) **264**, 698–701 (1967)
19. J. Vanier, R.F.C. Vessot: IEEE J. Quant. Elec. **9**, 391–398 (1966)
20. S. Dushman: Scientific foundations of vacuum technique, 2nd ed. New York: John Wiley and Sons Inc., 1966
21. M. Desaintfuscien, J. Viennet, C. Audoin: Metrologia **13**, 125–130 (1977)
22. P.L. Bender: Phys. Rev. **132**, 2154–2158 (1963)
23. L.C. Balling, R.J. Hanson, F.M. Pipkin: Phys. Rev. **A33**, 607–626 (1964)
24. H.C. Berg: Phys. Rev. **137**, 1621–1634 (1965)
25. O. Gheorghiu, J. Viennet, P. Petit, C. Audoin: C.R. Acad. Sci. (France), **V278**, 109–116 (1974)
26. R. Brousseau, J. Vanier: IEEE Trans. Instrum. Meas. **22**, 367–376 (1973)
27. D. Morris, K. Nakagiri: Metrologia **12**, 1–6 (1976)
28. C. Audoin, P. Lesage, J. Viennet, R. Barillet: IEEE Trans. Instrum. Meas. **29**, 98–104 (1980)
29. P. Petit, J. Viennet, R. Barillet, M. Desaintfuscien, C. Audoin: Metrologia **10**, 61–67 (1974)
30. N. Beverini, J. Vanier: IEEE Trans. Instrum. Meas. **28**, 100–104 (1979)
31. S.B. Crampton, D. Kleppner, N.F. Ramsey: Phys. Rev. Lett. **11**, 338–340 (1963)
32. J. Vanier, R.F.C. Vessot: Appl. Phys. Lett. **4**, 122–123 (1964)
33. S.B. Crampton, H.T.M. Wang: Phys. Rev. **A-12**, 1305–1312 (1975)
34. M. Desaintfuscien, J. Viennet, C. Audoin, J. Vanier: J. Phys. Lett. **36**, 281–284 (1975)
35. S.B. Crampton, E.C. Fleri, H.T.M. Wang: Metrologia **13**, 131–135 (1977)
36. D. Morris: IEEE Trans. Instr. Meas. **IM-31**, 88–91 (1982)
37. S.A. Wolf, D.U. Gubser, J.E. Cox: Shielding of longitudinal magnetic fields with thin, closely spaced, concentric cylindrical shells, with applications to atomic clocks. Proc. 10th Annual Precise Time and Time Interval (PTTI) Applications and Planning Meeting, pp. 131–146, 1978. (NASA, Goddard Space Flight Center, Greenbelt, Md)
38. D.E. Gubser, S.A. Wolf, J.E. Cox: Rev. Sci. Instrum. **50**, 751–756 (1979)
39. J. Vanier, G. Racine, R. Kunski, M. Picard: Progress report on hydrogen maser development at Laval university. Proc. 12th Annual Precise Time and Time Interval (PTTI) Applications and Planning Meeting, pp. 807–824, 1980. (NASA, Goddard Space Flight Center, Greenbelt, Md)
40. J. Vanier, R.F.C. Vessot: Metrologia **6**, 52–53 (1970)
41. P.W. Zitzewitz, E.E. Uzgiris, N.F. Ramsey: Rev. Sci. Instrum. **41**, 81–86 (1970)
42. D. Morris: Metrologia **7**, 162–166 (1971)
43. Y.M. Cheng, Y.L. Hua, C.B. Chen, J.H. Gao, W. Shen: IEEE Trans. Instrum. Meas. **29**, 316–319 (1980)
44. J. Vanier, R. Larouche, C. Audoin: The hydrogen maser wall shift problem. Proc. 29th Annual Symp. Frequency Control, pp. 371–382, 1975. USAEC Fort Monmouth, NJ (Electronic Industries Association, 2001 Eye Street N.W., Washington D.C.)
45. R.F.C. Vessot, M.W. Levine: Metrologia **6**, 116–117 (1970)
46. P.W. Zitzewitz: Surface collision frequency shifts in the atomic hydrogen maser. Proc. 24th Annual Symp. Frequency Control, pp. 263–267, 1970. USAEC Fort Monmouth, NJ (Electronic Industries Association, 2001 Eye Street N.W., Washington D.C.)
47. P.E. Debely: Hydrogen maser with deformable storage bulb. Proc. 24th Ann. Symp. Frequency Control, pp. 259–261, 1970. USAEC Fort Monmouth, NJ (Electronic Industries Association, 2001 Eye Street N.W., Washington D.C.)
48. V.S. Reinhardt: Variable volume maser techniques. Proc. 8th Annual Precise Time and Time Interval (PTTI) Applications and Planning Meeting, pp. 335–350, 1976. (NASA, Goddard Space Flight Center, Greenbelt, Md)
49. P. Petit, M. Desaintfuscien, C. Audoin: Hydrogen maser with a double configuration bulb for wall shift measurements in the temperature range 25–120 °C. Proc. 31st Ann. Symp. Freq. Control, pp. 520–524, 1977. USAEC Fort Monmouth, NJ (Electronic Industries Association, 2001 Eye Street N.W., Washington D.C.)
50. D. Morris: IEEE Trans. Instr. Meas. **27**, 339–343 (1978)
51. J.A. Barnes, A.R. Chi, L.S. Cutler, D.J. Healy, D.B. Leeson, T.E. McGunigal, J.A. Mullen, W.Z. Smith, R.L. Sydnor, R.F.C. Vessot, G.M.R. Winkler: IEEE Trans. Instrum. Meas. **20**, 105–120 (1971)
52. R.F.C. Vessot, L. Mueller, J. Vanier: Proc. IEEE **54**, 199–207 (1966)
53. L.S. Cutler, C.L. Searle: Proc. IEEE **54** , 136–154 (1966)
54. R.F.C. Vessot, M.W. Levine, E.M. Mattison: Comparison of theoretical and observed hydrogen maser stability limitation due to thermal noise and the prospect for improvement by low-temperature operation. Proc. 9th Annual Precise Time and Time Interval (PTTI) Applications and Planning Meeting, pp. 549–569, 1977. (NASA, Goddard Space Flight Center, Greenbelt, Md)
55. R.F.C. Vessot, M.W. Levine, P.W. Zitzewitz, P. Debely, N.F. Ramsey: Recent developments affecting the hydrogen maser as a frequency standard. NBS Special Publication 343 Precision Measurement and Fundamental Constants, U.S. Department of Commerce, National Bureau of Standards, pp. 27–38, 1971
56. J. Vanier, L.G. Bernier, M. Têtu: IEEE Trans. Inst. Meas. **28**, 188–193 (1979)
57. J. Vanier, M. Têtu: IEEE Trans. Com. Special Issue on Phase-Locked Loops. Oct. 1982. Part 1
58. R.F.C. Vessot, E.M. Mattison, E.L. Blomberg: Research with a cold atomic hydrogen maser. Proc. 33rd Ann. Symp. Frequency Control, pp. 511–514, 1979. USAEC Fort Monmouth, N.J. (Electronic Industries Association, 2001 Eye Street N.W., Washington D.C.)
59. W.N. Hardy, M. Morrow, R. Jochemsen, B.W. Statt, P.R. Kubik, R.M. Marsolais, A.J. Berlinsky: Phys. Rev. Lett. **45**, 453–456 (1980)
60. S.B. Crampton: Phys. Rev. Lett. **42**, 1039–1041 (1979)
61. S.B. Crampton: J. Phys. **41**, Colloq. C7, 249–255 (1980)
62. C. Audoin, P. Lesage, J. Viennet, R. Barillet: Analysis of H maser autotuning systems. Proc. 32nd Ann. Symp. Frequency Control, pp. 531–541, 1978. USAEC Fort Monmouth, NJ (Electronic Industries Association, 2001 Eye Street N.W., Washington D.C.)

63. E.M. Mattison, M.W. Levine, R.F.C. Vessot: New TE_{111}-mode hydrogen maser. Proc. 8th Annual Precise Time and Time Interval (PTTI) Applications and Planning Meeting, pp. 355–367, 1976. (NASA, Goddard Space Flight Center, Greenbelt, Md)
64. H.E. Peters: Small, very small, and extremely small hydrogen masers. Proc. 32nd Ann. Symp. on Freq. Control, pp. 469–476, 1978. USAEC Fort Monmouth NJ (Electronic Industries Association, 2001 Eye Street N.W., Washington D.C.)
65. H.E. Peters: Feasibility of extremely small hydrogen masers. Proc. 35th Ann. Symp. on Freq. Control, pp. 662–666, 1981. USAERADCOM Fort Monmouth NJ (Electronic Industries Association, 2001 Eye Street N.W., Washington D.C.)
66. H.T. Wang: An oscillating compact hydrogen maser. Proc. 34th Ann. Symp. on Freq. Control, pp. 364–369, 1980. USAEC Fort Monmouth, NJ (Electronic Industries Association, 2001 Eye Street N.W., Washington D.C.)
67. P.R. Dachel, R.F. Meyer, S.M. Petty, R.L. Sydnor: Hydrogen maser frequency standards for the deep space network. Proc. 8th Ann. Precise Time and Time Interval (PTTI) Applications and Planning Meeting, pp. 213–228, 1976. (NASA, Goddard Space Flight Center, Greenbelt, Md)
68. D.W. Curkendall: PTTI applications to deep space navigation. Proc. 10th Annual Precise Time and Time Interval (PTTI) Applications and Planning Meeting, pp. 659–692, 1978. (NASA, Goddard Space Flight Center, Greenbelt, Md)
69. P.F. Kuhnle: Hydrogen maser implementation in the deep space network at the Jet Propulsion Laboratory. Proc. 11th Precise Time and Time Interval (PTTI) Applications and Planning Meeting, pp. 197–212. 1979. (NASA, Goddard Space Flight Center, Greenbelt, Md)
70. T.H. Legg, N.W. Broten, D.N. Fort, J.L. Yen, F.V. Bale, P.C. Barker, M.J.S. Quigley: Nature **244**, 18–19 (1973)
71. N.W. Broten, T.H. Legg, J.L. Loche, C.W. McLeish, R.S. Richards, R.M. Chisholm, H.P. Gush, J.L. Yen, J.A. Galt: Science **156**, 1592–1593 (1967)
72. T.A. Clark, I.I. Shapiro: Time geodesy and astrometry: results from radio interferometry. Proc. 5th Annual Precise Time and Time Interval (PTTI) Applications and Planning Meeting, pp. 33–46, 1973. (NASA, Goddard Space Flight Center, Greenbelt, Md)
73. A.R. Whitney, A.E.E. Rogers, H.F. Hinteregger, L.B. Hanson, T.A. Clark, C.C. Counselman III, I.I. Shapiro: Application of very long base line interferometry to astrometry and geodesy; effects of frequency standard instability on accuracy. Proc. 6th Annual Precise Time and Time Interval (PTTI) Applications and Planning Meeting, pp. 349–357, 1974. (NASA, Goddard Space Flight Center, Greenbelt, Md)
74. W.H. Cannon, R.B. Langley, W.T. Petrachenko: Clock rate comparisons by long base line interferometry. Proc. 9th Annual Precise Time and Time Interval (PTTI) Applications and Planning Meeting, pp. 113–126, 1977. (NASA, Goddard Space Flight Center, Greenbelt, Md)
75. A.E.E. Rogers, A.R. Whitney, H.F. Hinteregger, C.A. Knight, T.A. Clark, W.J. Klepczynski, I.I. Shapiro, C.C. Counselman: Clock synchronization via very long base line interferometry. Proc. 9th Annual Precise Time and Time Interval (PTTI) Applications and Planning Meeting, pp. 127–134, 1977 (NASA, Goddard Space Flight Center, Greenbelt, Md)
76. D. Morris, K. Nakagiri: Metrologia **12**, 1–6 (1976)
77. O. Gheorghiu, L. Giurgiu, F. Dragos, C. Mandache, T. Bocaniciu: J. Phys. **42**, Colloq. C8, 519 (1981) [title only]
78. R.F.C. Vessot, M.W. Levine: Gravitational redshift space-probe experiments. GP-A Project Final Report Contract NAS8-27969 Smithsonian Institution Astrophysical Observatory, Cambridge, MA 02138, USA
79. P. Petit, J. Viennet, R. Barillet, M. Desaintfuscien, C. Audoin: Hydrogen maser design at the Laboratoire de l'Horloge Atomique. Proc. 8th Ann. Precise Time and Time Interval (PTTI) Applications and Planning Meeting, pp. 229–248, 1976. (NASA, Goddard Space Flight Center, Greenbelt, Md)
80. L.J. Rueger, A. Bates, L. Stillman, J. Norton, C.M. Blackburn, V.A. Reinhardt: NASA NR hydrogen maser. Proc. 32nd Ann. Symp. Frequency Control, pp. 486–491, 1978. USAEC Fort Monmouth, NJ (Electronic Industries Association, 2001 Eye Street N.W., Washington D.C.)
81. L.J. Rueger: Characteristics of NASA research maser. Int. Symp. on Time and Frequency, New Delhi, India, 1981 (unpublished)
82. M.W. Levine, R.F.C. Vessot, E.M. Mattison, E. Blomberg, T.E. Hoffman, G. Nystrom, D.F. Graveline, R.L. Nicoll, C. Dovidio, W. Brymer: A hydrogen maser design for ground applications. Proc. 8th Ann. Precise Time and Time Interval (PTTI) Applications and Planning Meeting, pp. 249–276, 1976. (NASA, Goddard Space Flight Center, Greenbelt, Md)
83. C.H. Chuang, T.C. Jair: IEEE Trans. Instrum. Meas. **29**, 158–167 (1980)
84. X.B. Zhong, Q.J. Xu, S.Q. Yang, X.Z. Zeng: The hydrogen masers at Wuhan Institute of Physics. 1980 (unpublished)
85. Y. Ohta, K. Yoskimura, M. Shibuki, K. Nakagiri, T. Morikawa, M. Kobayaski, Y. Saburi: On an automatic cavity tuner for hydrogen frequency standard. 1974 (unpublished); S. Okamura: Report of the National Committee of Japan at URSI General Assembly Meeting, Lima, Peru, 1975 (unpublished)
86. H.T.M. Wang, J.B. Lewis, S.B. Crampton: Compact cavity for hydrogen frequency standards. Proc. 33rd Ann. Symp. Freq. Control, pp. 543–548, 1979. USAEC, Fort Monmouth, NJ (Electronic Industries Association, 2001 Eye Street N.W., Washington D.C.)
87. L. Essen, R.W. Donaldson, E.G. Hope, M.J. Bangham: Metrologia **9**, 128–137 (1973)
88. O.C. Gheorghiu, L.C. Giurgiu: Rev. Roum. Phys. **20**, 305–307 (1975)
89. S.B. Pouchkine, V. Sagine: Compte rendu de la 8ème session du Comité Consultatif pour la Définition de la Seconde. Bureau International des Poids et Mesures, Pavillon de Breteuil, F-92310, Sevres, France, pp. 389–393, 1977
90. G. Busca, F. Addor, F. Hadorn, G. Nicolas, L. Prost, H. Brandenberger, P. Thomann: Preliminary measurements of EFOS I H maser. 36th Ann. Symp. Freq. Cont. 1–4 june 1982. Philadelphia. (USAERADCOM Fort Monmouth NJ)
91. L.U. Hibbard: Elect. Electron. Eng. **1**, 243 (1981)